# 3D DoA-based Localization with Phase Jump Corrections

Hoang. M. Le[1,2], Dirk Slock[1], Jean-Pierre Rossi[2]

[1]Communication Systems Departement, EURECOM - Sophia Antipolis, France
[2]Orange Labs - Sophia Antipolis, France
Email: hoangminh.le@orange.com, leho@eurecom.fr

***Abstract*—Localizing a source based on the directions of its signals is an attractive approach because no synchronization among clocks is required. In this paper, we propose a Maximum Likelihood (ML) estimator to solve the location problem in 3D schemes, where a signal's direction is mathematically expressed by an elevation angle and an azimuth angle which applies iterative procedures for position estimation. This estimator applies iterative procedures for position estimations. To avoid confusions, the value of each angle must be predefined in an interval of $2\pi$-length. However, the convergence of iterative procedures will be really challenging if there are angle estimation errors caused by noisy measurements with values near the boundaries of this interval. In our proposed procedure, the elevation angle is defined with the arctan function and the azimuth angle is defined with the atan2 function, whose codomain is $2\pi$-long, to map the DoA. Furthermore, to robustify the estimations near the boundaries, phase jump corrections are proposed to rectify the final estimates. Simulation results show significant performance improvements.**

***Index Terms* -direction-based, positioning, DoA, Direction of Arrival, 3D localization, Maximum Likelihood.**

## I. Introduction

Localization in 3D is an important research field in wireless communications. So far, there are some principal positioning methods: Received Signal Strength (RSS), Time of Arrival (ToA), Time Difference of Arrival (TDoA), and Direction of Arrival (DoA) (in some other documents, it is often referred to as Angle of Arrival - AoA) [1]. RSS-based localization [2], [3] is very sensitive to the log normal fadings so it provides rough estimates for localization. On the other hand, in ToA-based [4]–[6] and TDoA-based [7]–[9] positioning, very accurate clock synchronization among all BSs and mobile device is highly demanded. DOA-based localization is an attractive approach, since no synchronization is required. The main challenge to this approach is that the accuracy of DoA estimations depend on the number of elements in the antenna array, their inter-element spacings and the Signal-to-Noise Ratio (SNR). Nevertheless, recent developments enable small antenna arrays with lower separation among the elements [10], which encourages the researches on position location using DoA.

As for localization based on ToA, TDoA, RSS, the positioning algorithms for 2D and 3D scenarios are quite similar. On the other hand, DoA-based positioning algorithm changes when we expand the 2D problems into 3D, because of the mathematical expression of DoA. An angle expressed a DoA in 2D schemes; meanwhile in 3D, each DoA is expressed by an azimuth angle and an elevation angle (Fig. 1).

### A. Related works

Fig. 1 demonstrates that at the $i$-th base station, the DoA of the incident wave is expressed by the azimuth angle $\varphi_i$ and an elevation angle $\theta_i$.

- The elevation angle $\theta_i$ is the trigonometric angle between the horizontal $(xy)$-plane and the incident wave. Its value varies from $-\pi/2$ to $\pi/2$.
- The azimuth angle $\varphi_i$ is the trigonometric angle between the $x$-direction and the orthogonal projection of the incident wave onto the $(xy)$-plane (Fig. 2). When $\alpha$ is the value of an angle, $\alpha + k2\pi$ (where $k$ is any integer) identifies the same angle, which will cause confusions in taking the estimated value of an angle. As a result, to avoid such a trouble, the set of definition of an azimuth angle must be in an interval of $2\pi$-length.

In practice, there are always additive noises in measured values of azimuth and elevation angles. At the boundaries of the sets of definition, the computations and estimations are very sensitive to noise:

- When the value of $\theta_i$ near the boundaries $-\pi/2$ or $\pi/2$, a small noise in measurements can make the calculation $\tan\theta_i$ considerably incorrect.
- As for $\varphi_i$, a small angle estimation error can lead to big consequences. On condition that the azimuth's set of definition is $[0;2\pi)$, when the true value of an angle is $\widehat{aOb} = \varepsilon_a$, a small error of $\varepsilon_a + \varepsilon_b$ (where $\varepsilon_a$ and $\varepsilon_b$ are small positive values) can make the angle's measured value $\widehat{aOb'} = 2\pi - \varepsilon_b$ (Fig. 3).

Related papers [11]–[15] about DoA-based localization use arctan function to define azimuth and elevation angles; meanwhile the codomain of that function is $[-\pi/2;\pi/2]$. This codomain does not comprise all the possible values of an azimuth angle. In the paper [16], a Maximum Likelihood estimator is proposed to optimize the positioning. However, the sensitivity to noise of a value near the boundaries of the set of definition of azimuth angles is not well considered and analysed.

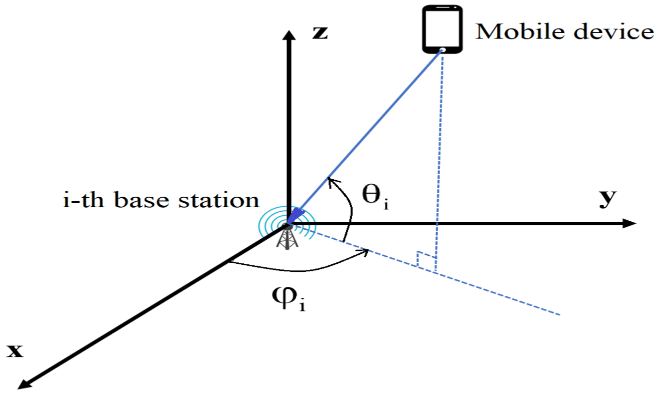


Fig. 1: Uplink DoA at the i-th base station in the xyz coordinate system

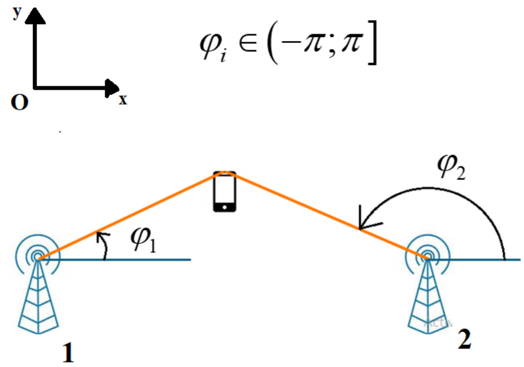


Fig. 2: Azimuth angles in noiseless scenario

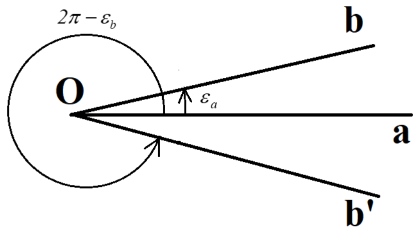


Fig. 3: Sensitivity to noise of an angle's measured value

### *B. Our contributions*

In this paper, we propose an algorithm that solves the problems of the sensitivity to noise.

- The azimuth angle is computed with atan2 function instead of arctan function. A modulo operation is applied to map the definition of azimuth. Furthermore, compared to [16], we formulate the Maximum Likelihood estimator, with a phase jump correction added in estimating azimuth angles to avoid possible huge computing errors caused by small mistakes in practical measurements.

With the assumptions above, it is rational to do localizing computations with estimated value of azimuth and elevation angles in section II. In section III, a Maximum Likelihood estimator is applied to optimize the position estimation. Furthermore, an additional correction is added in estimating the estimated azimuth angles to avoid possible huge computing errors caused by small mistakes in practical measurements.

Notations: $x$ can be the variable or the true value, depending on the context. $\hat{x}$ is the estimated value of $x$. $\mathbf{mod}(x,a)$ denotes $x$ modulo $a$; $\mathbf{diag}(a_1, a_2, \ldots, a_n)$ is the diagonal matrix whose diagonal elements are $a_1, a_2, \ldots, a_n$ respectively; $[a;b)$ is the interval of real numbers from $a$ to $b$ which includes $a$ but excludes $b$, **atan2** means 2-argument which is defined as: $\varphi = \text{atan2(y, x)} \iff \text{x + jy} = \text{r}e^{j\varphi}$ with $\text{r} = \sqrt{\text{x}^2+\text{y}^2}$, $\varphi \in (-\pi;\pi]$ and j is the imaginary unit. The standard arctangent function **arctan** has values in $[-\frac{\pi}{2}, \frac{\pi}{2}]$. Let

$$\text{sign}(x) = \begin{cases} 1 & , x \geq 0 \\ -1 & , x < 0 \,. \end{cases} \tag{1}$$

Then for $(x,y) \neq (0,0)$, we have

$$\text{atan2}(y,x) = \arctan\left(\frac{y}{x}\right) - (\text{sign}(x)-1)\,\text{sign}(y)\,\frac{\pi}{2}\,. \tag{2}$$

which takes values in $(-\pi;\pi]$.

## II. DoA-based Localization by Least Squares Algorithm

### *A. Definition of DoA*

Let $(x,y,z)$ be the coordinates of the mobile device and $(x_i,y_i,z_i)$ the coordinates of the $i$-th base station. An azimuth angle is a horizontal angle measured anticlockwise from the $x$-direction. Therefore, its value is in the interval $[0;2\pi)$. We then have the true azimuth of DoA of the signal to the $i$-th base station:

$$\varphi_i = \text{mod}(\text{atan2}(y-y_i, x-x_i), 2\pi) \tag{3}$$

Since the codomain of atan2 function is $(-\pi;\pi]$, a modulo operation with the divisor of $2\pi$ is applied to make the true value $\varphi_i$ in the interval $[0;2\pi)$.

In practical measurements, there are always errors in azimuth estimations. When the size of the angle is near to 0 or $2\pi$, the measured value is very sensitive to noise (a small change in noise can cause a big difference in measured value). To avoid this unexpected difference, a phase jump correction is applied. Consequently, the measured value of $i$-th azimuth angle can be expressed as:

$$\hat{\varphi}_i = \varphi_i + n_{az,i} + k_i 2\pi \tag{4}$$

where $n_{az,i}$ is the error in azimuth estimation. We name the action of adding the phase jump correction of $k_i 2\pi$ as **k-correction**. We then have the expression of $k_i$.

$$k_i = \begin{cases} 1 & , \varphi_i + n_{az,i} < 0 \\ -1 & , \varphi_i + n_{az,i} \geq 2\pi \\ 0 & \quad \text{otherwise.} \end{cases} \tag{5}$$

Thanks to the **k-correction**, the estimated azimuth angle is also in the interval: $0 \leq \hat{\varphi}_i < 2\pi$.

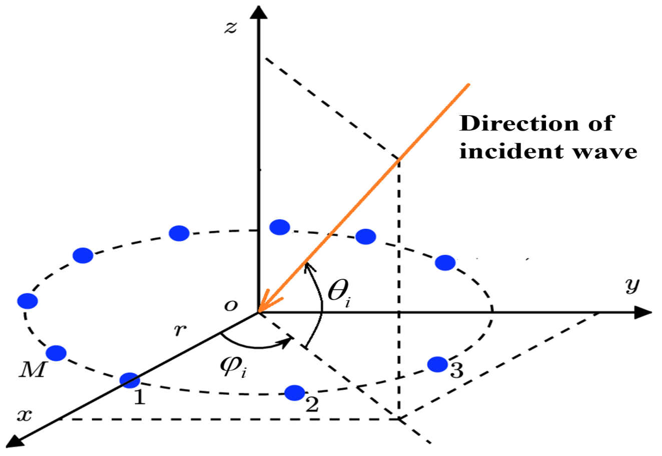


Fig. 4: $M$-element Uniform Circular Array (UCA) with radius $r$ at the $i$-th base station to estimate azimuth angle $\varphi_i$ and elevation angle $\theta_i$

As for the $i$-th elevation angle, its true value is expressed as:

$$\theta_i = \arctan \frac{z - z_i}{\sqrt{(x-x_i)^2 + (y-y_i)^2}} \quad (6)$$

The true elevation angle is in the range of $[-\pi/2; \pi/2]$, or $-\pi/2 \leq \theta_i \leq \pi/2$. Its measured value is

$$\hat{\theta}_i = \theta_i + n_{el,i} \quad (7)$$

where $n_{az,i}$ is the error in elevation estimation. When $\theta_i$ is far enough from the 2 boundaries of the interval $[-\pi/2, \pi/2]$ and $n_{el,i}$ is small enough, the estimated value $\hat{\theta}_i$ of the elevation angle can be considered to be also in this interval: $-\pi/2 \leq \hat{\theta}_i \leq \pi/2$.

At each base station, an $M$-element Uniform Circular Array (UCA) is installed to estimate the azimuth angle and the elevation angle of the incident wave (Fig. 4). In [17], it is proved that if noises in received signals are Gaussian distributed, $n_{az,i}$ and $n_{el,i}$ will be asymptotically and independently Gaussian distributed with zero-mean. Consequently, we can assume that $n_{az,i}$ and $n_{el,i}$ are independently Gaussian distributed with zero-mean. Their variances are $\sigma^2_{az,i}$ and $\sigma^2_{el,i}$, correspondingly.

Since all $n_{az,i}$ and $n_{el,i}$ are independent, we have covariance matrix of the noise vector $\boldsymbol{n}$:

$$\boldsymbol{C} = E\{\boldsymbol{n}\boldsymbol{n}^T\} = \mathrm{diag}\{\sigma^2_{az,1}, \ldots, \sigma^2_{az,N}, \sigma^2_{el,1}, \ldots, \sigma^2_{el,N}\} \quad (8)$$

where $\boldsymbol{n} = [n_{az,1} \;\ldots\; n_{az,N} \; n_{el,1} \;\ldots\; n_{el,N}]^T$ and $N$ is the number of base stations.

### B. Estimating position by Least Squares method

From equation (3), we have

$$\tan \varphi_i = \frac{y - y_i}{x - x_i} \quad (9)$$

$$x \sin \varphi_i - y \cos \varphi_i = x_i \sin \varphi_i - y_i \cos \varphi_i \quad (10)$$

As $n_{az,i}$ is very small, we approximate that $\sin n_{az,i} \approx 0$ and $\cos n_{az,i} \approx 1$. Thus

$$\sin \varphi_i = \sin(\hat{\varphi}_i - n_{az,i} - k_i 2\pi) = \sin(\hat{\varphi}_i - n_{az,i}) \approx \sin \hat{\varphi}_i \quad (11)$$

$$\cos \varphi_i = \cos(\hat{\varphi}_i - n_{az,i} - k_i 2\pi) = \cos(\hat{\varphi}_i - n_{az,i}) \approx \cos \hat{\varphi}_i \quad (12)$$

Hence, from (10), it is approximated that

$$x \sin \hat{\varphi}_i - y \cos \hat{\varphi}_i = x_i \sin \hat{\varphi}_i - y_i \cos \hat{\varphi}_i \quad (13)$$

From equation (6), we have

$$\tan \theta_i = \frac{z - z_i}{\sqrt{(x-x_i)^2 + (y-y_i)^2}} = \frac{(z - z_i)\cos \varphi_i}{x - x_i} \quad (14)$$

As $n_{el,i}$ is very small, we approximate that $\sin n_{el,i} \approx 0$ and $\cos n_{az,i} \approx 1$, so $\tan n_{el,i} \approx 0$. Thus $\tan \theta_i \approx \tan \hat{\theta}_i$

We have the approximation

$$\tan \hat{\theta}_i = \frac{(z - z_i)\cos \hat{\varphi}_i}{x - x_i} \quad (15)$$

$$x \tan \hat{\theta}_i - z \cos \hat{\varphi}_i = x_i \tan \hat{\theta}_i - z_i \cos \hat{\varphi}_i \quad (16)$$

In matrix approach

$$\hat{\boldsymbol{A}} = \begin{bmatrix} \sin \hat{\varphi}_1 & -\cos \hat{\varphi}_1 & 0 \\ \sin \hat{\varphi}_2 & -\cos \hat{\varphi}_2 & 0 \\ \ldots & \ldots & \ldots \\ \sin \hat{\varphi}_N & -\cos \hat{\varphi}_N & 0 \\ \tan \hat{\theta}_1 & 0 & -\cos \hat{\varphi}_1 \\ \tan \hat{\theta}_2 & 0 & -\cos \hat{\varphi}_2 \\ \ldots & \ldots & \ldots \\ \tan \hat{\theta}_N & 0 & -\cos \hat{\varphi}_N \end{bmatrix}$$

$$\hat{\boldsymbol{b}} = \begin{bmatrix} x_1 \sin \hat{\varphi}_1 - y_1 \cos \hat{\varphi}_1 \\ x_2 \sin \hat{\varphi}_2 - y_2 \cos \hat{\varphi}_2 \\ \ldots \\ x_N \sin \hat{\varphi}_N - y_N \cos \hat{\varphi}_N \\ x_1 \tan \hat{\theta}_1 - z_1 \cos \hat{\varphi}_1 \\ x_2 \tan \hat{\theta}_2 - z_2 \cos \hat{\varphi}_2 \\ \ldots \\ x_N \tan \hat{\theta}_N - z_N \cos \hat{\varphi}_N \end{bmatrix}$$

$$\boldsymbol{x} = \begin{bmatrix} x & y & z \end{bmatrix}^T$$

We then have the equation of approximation

$$\hat{\boldsymbol{A}}\,\boldsymbol{x} = \hat{\boldsymbol{b}} \quad (17)$$

Therefore, the estimate of $\boldsymbol{x}$ is

$$\hat{\boldsymbol{x}} = \min_{\boldsymbol{x}} \|\hat{\boldsymbol{A}}\boldsymbol{x} - \hat{\boldsymbol{b}}\|^2 \quad (18)$$

$\hat{\boldsymbol{x}}$ is calculated by Least-Square estimation of $\boldsymbol{x}$

$$\hat{\boldsymbol{x}} = \hat{\boldsymbol{A}}^{\dagger}\hat{\boldsymbol{b}} \quad (19)$$

where $\boldsymbol{A}^{\dagger} = (\boldsymbol{A}^T\boldsymbol{A})^{-1}\boldsymbol{A}^T$ is the Moore-Penrose pseudo inverse of matrix $\boldsymbol{A}$.

For a more accurate estimation of the mobile's position, this estimate is taken as the initialization of an iterative procedure, which will be discussed in the following section.

## III. Optimizing position estimation by the true Maximum Likelihood estimator

In this section, we apply an iterative Maximum Likelihood estimator, to optimize $\hat{\boldsymbol{x}}$ obtained in (19),

In vector form, we denote

$$\hat{\boldsymbol{\varphi}} = \begin{bmatrix} \hat{\varphi}_1 & \dots & \hat{\varphi}_N & \hat{\theta}_1 & \dots & \hat{\theta}_N \end{bmatrix}^T \tag{20}$$

$$\boldsymbol{f}(\boldsymbol{x},\boldsymbol{k}) = \begin{bmatrix} \varphi_1(\boldsymbol{x}) + k_1 2\pi \\ \varphi_2(\boldsymbol{x}) + k_2 2\pi \\ \dots \\ \varphi_N(\boldsymbol{x}) + k_N 2\pi \\ \theta_1(\boldsymbol{x}) \\ \theta_2(\boldsymbol{x}) \\ \dots \\ \theta_N(\boldsymbol{x}) \end{bmatrix} \tag{21}$$

where $\boldsymbol{k} = [k_1 \; k_2 \; \cdots \; k_N]^T$; $\varphi_i(\boldsymbol{x})$ and $\theta_i(\boldsymbol{x})$ are the estimated azimuth and elevation angles, respectively, depending on $\boldsymbol{x} = [x \;\; y \;\; z]^T$ and are computed by

$$\varphi_i(\boldsymbol{x}) = \mathrm{mod}(\mathrm{atan2}(x - x_i,\; y - y_i), 2\pi) \tag{22}$$

$$\theta_i(\boldsymbol{x}) = \arctan \frac{z - z_i}{\sqrt{(x - x_i)^2 + (y - y_i)^2}} \tag{23}$$

Treating the phase shift vector $\boldsymbol{k}$ as unknown parameters and ignoring their dependence on the noise, the measurement vector $\hat{\boldsymbol{\varphi}}$ is Gaussian with mean vector of $\boldsymbol{f}$ and covariance matrix $\mathrm{C}_u$, we have the probability density function (pdf) [18]:

$$\mathrm{p}(\hat{\boldsymbol{\varphi}}|\boldsymbol{x},\boldsymbol{k}) = \frac{(2\pi)^{-N}}{|\boldsymbol{C}|^{1/2}} \exp\left[\frac{-1}{2}(\hat{\boldsymbol{\varphi}} - \boldsymbol{f})^T \mathrm{C}^{-1}(\hat{\boldsymbol{\varphi}} - \boldsymbol{f})\right] \tag{24}$$

Maximizing the pdf in (24) is equivalent to

$$\hat{\boldsymbol{x}}, \widehat{\boldsymbol{k}} = \arg\min_{\boldsymbol{x},\boldsymbol{k}} (\hat{\boldsymbol{\varphi}} - \boldsymbol{f}(\boldsymbol{x},\boldsymbol{k}))^T \boldsymbol{C}^{-1} (\hat{\boldsymbol{\varphi}} - \boldsymbol{f}(\boldsymbol{x},\boldsymbol{k})) \tag{25}$$

which we shall perform alternatingly. We consider Gauss Newton [19] for $\hat{x}$. At the iteration $(u+1)$:

$$\hat{\boldsymbol{x}}^{(u+1)} = \hat{\boldsymbol{x}}^{(u)} + (\boldsymbol{G}^T \boldsymbol{C}^{-1} \boldsymbol{G})^{-1} \boldsymbol{G}^T \boldsymbol{C}^{-1} (\hat{\boldsymbol{\varphi}} - \boldsymbol{f}(\hat{\boldsymbol{x}}^{(u)}, \boldsymbol{k}^{(u+1)})) \tag{26}$$

where $\boldsymbol{G}$ is the Jacobian matrix.

$$\boldsymbol{G} = \boldsymbol{G}(\hat{\boldsymbol{x}}^{(u)}, \boldsymbol{k}^{(u+1)}),\; \boldsymbol{G}(\boldsymbol{x},\boldsymbol{k}) = \frac{\partial \boldsymbol{f}(\boldsymbol{x},\boldsymbol{k})}{\partial \boldsymbol{x}^T}. \tag{27}$$

At this point, it is important to determine the value of $k_i$. As the additive noise in each DoA measurement is unclear, $k_i$ cannot be determined by equation (5). From (4), we have

$$|n_{az,i}| = |\hat{\varphi}_i - \varphi_i(\boldsymbol{x}) - k_i 2\pi| \tag{28}$$

We assume $n_{az,i}$ small enough, so $|n_{az,i}| < \pi$ with the probability almost 1. Thus $\widehat{k_i}$ can be estimated by

$$\hat{k}_i^{(u+1)} = \arg\min_{k_i \in \{0;\pm 1\}} |\hat{\varphi}_i - \varphi_i(\hat{\boldsymbol{x}}^{(u)}) - k_i 2\pi| \tag{29}$$

where $\hat{\boldsymbol{x}}^{(u)}$ is the estimated coordinate vector of the mobile device at the $u$-th iteration.

The procedure is expected to terminate when $\|\hat{\boldsymbol{x}}^{(u)} - \hat{\boldsymbol{x}}^{(u-1)}\|_2 < \varepsilon$, for the stopping value $\varepsilon$ sufficiently small. However, iterative procedures do not always converge. In [20], we show that there are **three** possible outcomes for an iterative procedure: **Convergence, Divergence** and **Oscillation**.

If a procedure is diverging or oscillation, we will take its initialization as the estimated mobile position. As for a converging procedure, the final position is selected as estimate.

In summary, the Algorithm 1, a Gauss-Newton iterative procedure of Maximum Likelihood estimator, is proposed.

**Algorithm 1:** Proposed Maximum Likelihood estimator with estimation of $\hat{\boldsymbol{k}}$

```
Take the measured Direction of Arrival: azimuth φ̂_i
   and elevation θ̂_i.
Assign u = 1 and ε sufficiently small.
Assign the coordinate vector computed by (19) as the
   first estimated coordinate vector x̂^(1) of the mobile
   device.
repeat
    Compute the estimated azimuth φ̂_i and elevation θ̂_i
      by (22) and (23), respectively.
    if |φ_i(x̂^(u)) − φ̂_i| ≥ π then
        k̂_i = sign(φ_i(x̂^(u)) − φ̂_i)
    else
        k̂_i = 0 ;
    Compute the following estimated coordinate vector
      x̂^(u+1) of the mobile device by (26).
    u = u + 1;
until ||x^(u) − x^(u−1)||_2 < ε or u > 1000 or
   ||x^(u)||_2 = ±∞;
if u > 1000 or ||x̂^(u)||_2 = ±∞ then
    x̂^(1) is the estimated position of the mobile device;
else
    x̂^(u) is the estimated position of the mobile device;
```

## IV. Simulations and Results

### A. Cramer-Rao Bound (CRB)

The Cramer-Rao Bound (CRB) is computed for the quaility evaluation of the algorithm. The Fisher Information Matrix (FIM) is calculated by

$$\boldsymbol{I}(\boldsymbol{x}) = \boldsymbol{G}^T(\boldsymbol{x}) \boldsymbol{C}^{-1} \boldsymbol{G}(\boldsymbol{x}) \tag{30}$$

The CRB is the trace of the inverse of FIM:

$$\mathrm{CRB} = \mathrm{tr}(\boldsymbol{I}^{-1}) \tag{31}$$

### B. Simulation Setup

The Root Mean Square Position Error (RMSE) is defined by

$$\mathrm{RMSE} = \sqrt{\mathrm{E}(\|\hat{\boldsymbol{x}} - \boldsymbol{x}\|^2)} \tag{32}$$

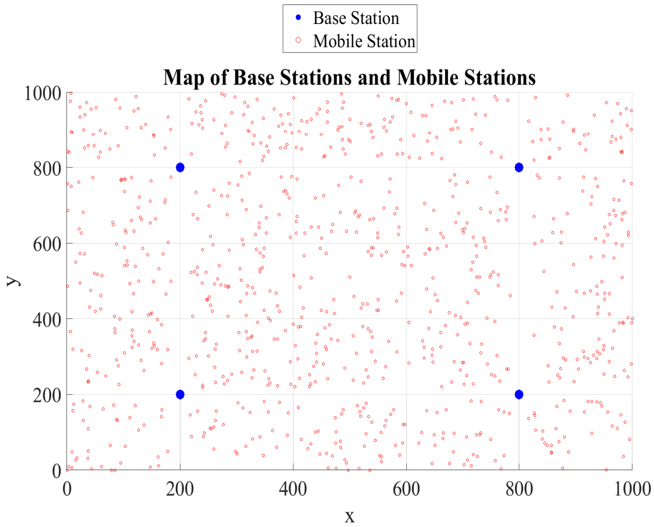


(a) View from top

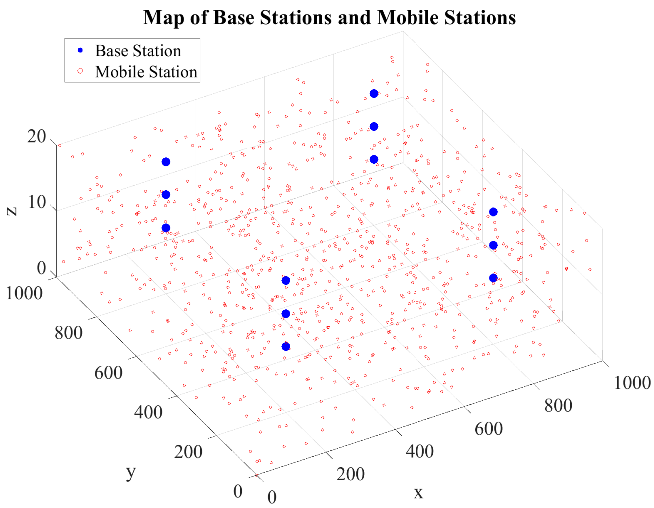


(b) View from one side

Fig. 5: Map of base stations and random positions of the mobile device

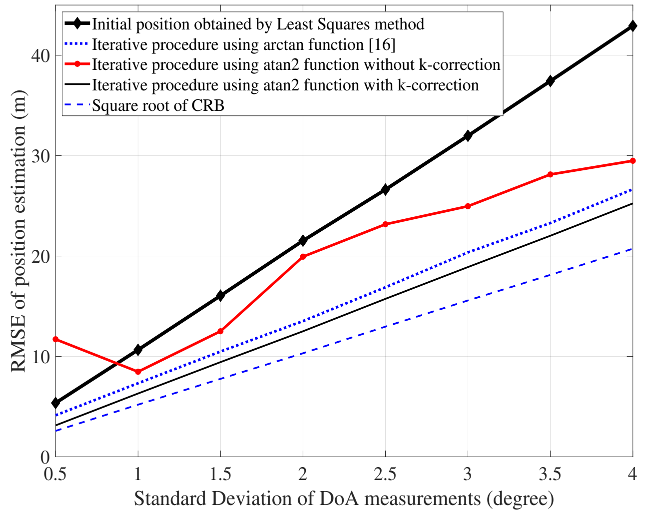


Fig. 6: DoA-based localization at network of base stations: Comparison of RMSE when the standard deviation of DoA measuremnts varies from 0.5° to 4°

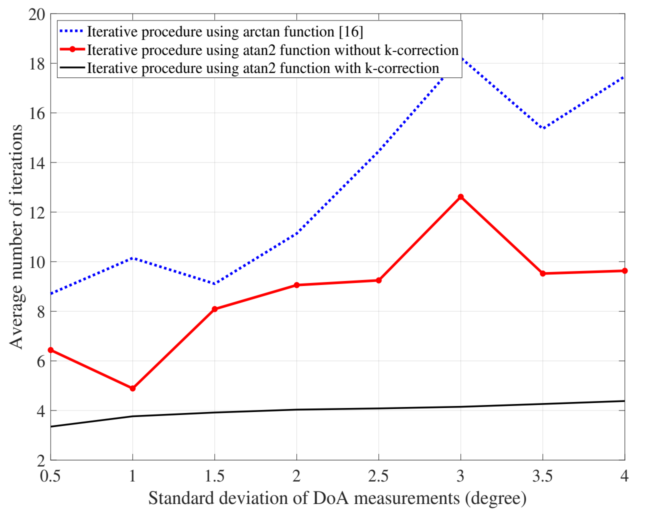


Fig. 7: DoA-based localization at network of base stations: Comparison of average number of iterations when the standard deviation of DoA measuremnts varies from 0.5° to 4°

where $\boldsymbol{x}$ is the true position of the mobile device and $\hat{\boldsymbol{x}}$ is its estimate.

We consider an area of 1000m x 1000m with the height of 20m. RMSE averaging is over 1000 mobile positions picked randomly in this space (Fig. 5). The center of this space is at the coordinates (500; 500; 10). At the height of 10m, 4 base stations of the coordinates (200; 200; 10), (800; 200; 10), (200; 800; 10) and (800; 800; 10) are placed, which forms a square. To enhance the localization in 3D, two similar sets of base stations are installed at the height of 15m and 20m, respectively. As a result, there are totally 12 base stations in our network.

The positions of the base stations, as well as the space where the mobile device is arbitrarily placed, are illustrated with a view from top (Fig. 5a) and a view from one side (Fig. 5b). In Fig. 5a, the x-coordinate and y-coordinate of any random position of the mobile device are set up to be far enough from those coordinates of all the base stations, so that the true elevation angles are far from the 2 boundaries $-\pi/2$ and $\pi/2$.

The value $\varepsilon$ for the stopping criterion is 0.01.

### C. Results

Instead of comparing the MSEs to the CRB, we compare their square roots: The Root Mean Square Error (RMSE) = $\sqrt{\text{MSE}}$ and square root of CRB ($\sqrt{\text{CRB}}$). In the simulations,

| Possible outcomes | Estimated position of mobile | RMSE | Number of iterations |
|---|---|---|---|
| Convergence | Final position of the procedure | Low | Low (fewer than 10) |
| Divergence | First position of the procedure | High | Low (fewer than 10) |
| Oscillation | First position of the procedure | High | High (1000) |

TABLE I: Possible outcomes of an iterative procedure

we assume that all the estimations of azimuth and elevation angles have the same standard deviation: $\sigma_{az,1} = \sigma_{el,1} = \cdots = \sigma_{az,N} = \sigma_{el,N} = \sigma$.

Fig. 6 and Fig. 7 illustrate the results when the common standard deviation of DoA estimations $(\sigma)$ varies from 0.5° to 4°. Specifically, Fig. 6 compares the RMSEs of the 4 algorithms:

(a) The initial position obtained by Least Squares method shown in section II-B.
(b) Maximum Likelihood estimator with the definition of azimuth angle using arctan function [16].
(c) Maximum Likelihood estimator **without** k-correction; the definition of azimuth angle using atan2 function without k-correction.
(d) Maximum Likelihood estimator **with** k-correction; the definition of azimuth angle using atan2 function (our proposed algorithm).

To validate the performances of the algorithms, we added the $\sqrt{CRB}$. Fig. 7 compares the average number of iterations of the three algorithms (b), (c) and (d).

Section III introduces 3 possible outcomes of an iterative procedure. Table I compares their results on RMSE and number of iterations.

In Fig. 6, the RMSE of our proposed algorithm (d) is much smaller than the "initial point" and higher than the $\sqrt{\text{CRB}}$, which shows that the algorithm (d) is efficient and unbiased. Compared to the algorithms (b) and (c), the algorithm (d) has the lowest RMSE so its positioning results are the most accurate. Furthermore, in Fig. 7, the average number of iterations of our proposed algorithm (d) is the lowest, which proves that this algorithm has the most converging procedures and the fewest combinations of diverging and oscillating procedures. As a result, it reduces remarkably the time delay for localization.

## V. Conclusions

This paper thoroughly analyzes a Maximum Likelihood estimator with the DoA-based positioning algorithms using the phase jump corrections and atan2 function to define the azimuth angle. The simulations demonstrate the superior properties of our proposed algorithm: maintaining the unbiased property with the most accurate results and the shortest time delay.

However, this positioning algorithm is only feasible for localization at network of base stations, where the orientation of the antenna array is already known and unchanged. The positioning algorithms for mobile-based localization, where the orientation of the mobile device is unknown, are under researches. An extension of [20] into 3D schemes, where mobile position is estimated based on Direction Difference of Arrival (DDoA), is a promising approach.


## Acknowledgment

EURECOM's research is partially supported by its industrial members: ORANGE, BMW, Symantec, SAP, Monaco Telecom, iABG. The Research of EURECOM and ORANGE was also supported in part by the French FUI project GEOLOC.


## References


[1] J. A. del Peral-Rosado, R. Raulefs, J. A. López-Salcedo, and G. Seco-Granados, "Survey of cellular mobile radio localization methods: From 1G to 5G," *IEEE Commun. Surveys Tuts.*, vol. 20, pp. 1124–1148, 2018.
[2] Q. Wang, Z. Duan, and X. R. Li, "Three-dimensional location estimation using biased RSS measurements," *IEEE Transactions on Aerospace and Electronic Systems*, vol. 56, 2020.
[3] C. Zhao, T. Yu, X. Tian, H. Yu, X. Gan, and X. Wang, "A 3-D RSS distribution model based on statistical properties for indoor localization systems," *IEEE/CIC International Conference on Communications in China (ICCC)*, 2015.
[4] M. I. ul Haq and D. Kim, "Improved localization by time of arrival for internet of things in 3D," *22nd International Conference on Applied Electromagnetics and Communications (ICECOM)*, 2016.
[5] D. Ni, O. A. Postolache, C. Mi, M. Zhong, and Y. Wang, "Uwb indoor positioning application based on kalman filter and 3-D toa localization algorithm," *11th International Symposium on Advanced Topics in Electrical Engineering (ATEE)*, 2019.
[6] W. Wang, Y. Zhang, and L. Tian, "TOA-based NLOS error mitigation algorithm for 3D indoor localization," *China Communications*, vol. 17, 2020.
[7] Z. Qin, J. Wang, and S. Wei, "A study of 3D sensor array geometry for TDOA based localization," *CIE International Conference on Radar (RADAR)*, 2016.
[8] M. Khalaf-Allah and S. U. Qaisar, "Nuisance parameter exploitation for accurate 3D hyperbolic geolocation - field results," *14th International Radar Symposium (IRS)*, 2013.
[9] H. Nabila, J. Suryana, and A. Izzuddin, "3D multilateration using rf burst," *6th International Conference on Wireless and Telematics (ICWT)*, 2020.
[10] D. Munoz, C. Vargas, R. Enriquez-Caldera, and F. B. Lara, *Position Location Techniques and Applications*, 2009.
[11] F. Wen, P. Liu, H. Wei, Y. Zhang, and R. C. Qiu, "Joint azimuth, elevation, and delay estimation for 3-D indoor localization," *IEEE Transactions on Vehicular Technology*, vol. 67, 2018.
[12] K. Dogancay and G. Ibal, "Instrumental variable estimator for 3D bearings-only emitter localization," *International Conference on Intelligent Sensors, Sensor Networks and Information Processing*, 2005.
[13] L. Badriasl and K. Dogancay, "Three-dimensional target motion analysis using azimuth/elevation angles," *IEEE Transactions on Aerospace and Electronic Systems*, vol. 50, 2014.
[14] Y. Ma and L. Jin, "Sensitivity analysis of DOA error on least square-based source localization in UWSAN," *7th International Congress on Image and Signal Processing*, 2014.
[15] S. Xu and K. Doğançay, "Optimal sensor deployment for 3D AOA target localization," *IEEE International Conference on Acoustics, Speech and Signal Processing (ICASSP)*, 2015.
[16] Y. Wang and K. C. Ho, "An asymptotically efficient estimator in closed-form for 3-D AOA localization using a sensor network," *IEEE Transactions on Wireless Communications*, vol. 14, 2015.
[17] A. Chan and J. Litva, "MUSIC and maximum likelihood techniques on two-dimensional DOA estimation with uniform circular array," *IEE Proc, Radar Sonar Navig*, vol. 142, no. 3, pp. 105–114, 1995.
[18] Y. L. Tong, *Fundamental Properties and Sampling Distributions of the Multivariate Normal Distribution*. Ed.Springer, 1989.
[19] A. Bjorck, *Numerical Methods for Least Squares Problems*. SIAM (Society for Industrial and Applied Mathematics), 1996.
[20] H. M. Le, D. Slock, and J.-P. Rossi, "2D DDoA-based self-positioning for mobile devices," *EUSIPCO*, 2021.